The Decay and Stability of Internal Wave Modes in a Multisheeted Thermocline[1]

Bryan Johns and Michael J. Cross

Department of Geophysics
Department of Mathematics
University of Reading
Reading, England

ABSTRACT

Internal wave motions are considered in a thermocline that consists of thin sheets across which there are abrupt changes in the density. These sheets are separated by homogeneous layers of water in which there is turbulent mixing. Investigations have been undertaken to determine the dependence of both the rate of energy dissipation and the dynamical stability upon the number of sheets in the thermocline. We have concluded that: (i) the higher-order internal wave modes are so heavily damped that they cannot persist as free oscillations for more than a few cycles; (ii) the dynamical stability of the internal modes is greatly increased by an increase in the number of sheets in the thermocline; (iii) for a specified number of sheets, the higher modes are less stable than the lower.

1. *Introduction.* The contributions of Woods and Fosberry (1967) concerning the fine structure of the thermocline have important implications in an understanding of internal-wave propagation. Their observations have indicated that the thermocline consists of a number of sheets, each having a thickness of a few centimeters; across these sheets there is an abrupt temperature (hence density) change. In the middle of these sheets, the water motion is laminar in a band having a thickness of a few millimeters, which indeed must be the case if the identity of the sheets is to be preserved. The sheets are separated by relatively much thicker layers of almost homogeneous water in which there are turbulent motions. These sheets contain regions of high shear relative to the adjacent layers, where the shears are much smaller.

In order to describe internal wave motions in such a structure, it seems appropriate to specify a discontinuous distribution of density in the thermocline in preference to a continuous profile. The density discontinuities correspond to the sheets and, as indicated by Johns and Cross (1969), these discontinuities lead to intense shear layers across which the water velocity rapidly adjusts its

1. Accepted for publication and submitted to press 26 January 1970.

value from one layer to the next. In the physical sense, then, we are prescribing that abrupt density changes occur across a distance equal to a sheet width as determined by the thickness of the shear layer. Within these shear layers there is energy dissipation that leads to the decay and ultimate disappearance of a free internal-wave oscillation. A scheme for determining this decay has been given by Johns and Cross (1969) in their formulation of a mathematical model that uses uniform coefficients of eddy viscosity to simulate the turbulent mixing in the layers. Their work indicates that, in certain circumstances, the internal waves may be heavily damped in comparison with the surface mode. Moreover, they have proposed that this decay is correspondingly enhanced by the addition of more sheets to the system.

The present paper develops more fully the above-mentioned ideas of Johns and Cross (1969) and applies them to an investigation of the decay and dynamical stability of internal-wave modes in thermoclines containing up to eight sheets. Some of the results are surprising at first and are contrary to our earlier speculations. With regard to the higher-order modes, our conclusions lead to a chain of interesting consequences that are discussed in § 3.

The theoretical development in this paper parallels that of Johns and Cross (1969). We have focused our attention upon a single Fourier component of the wave spectrum and have analyzed the dynamical processes in a system in which the Coriolis effects are omitted. The simplest thermocline consists of only two sheets at specified depths, with the sheets separated by a homogeneous layer of water. The total density change across this structure (attained in two abrupt jumps) is equal to $\Delta\varrho$. This system is then generalized by adding more sheets to the homogeneous layer between the two basic sheets, the latter retaining fixed identities throughout the process. The additional sheets are positioned so that the basic homogeneous layer is equally divided into homogeneous sublayers. The total density change across the thermocline remains equal to $\Delta\varrho$, this being attained by equal density jumps across each of the sheets.

2. *Mathematical Specification.* Conditions are referred to Cartesian axes (x, y) fixed within the mean level of the free surface, with the y axis vertically upward. The instantaneous positions of the centers of the N sheets in the thermocline are expressed by

$$y = -y_{n-1} + \eta_n; \qquad n = 2, 3, \ldots N+1, \tag{1}$$

where

$$\eta_n = a(\alpha_{0\,n-1} + \varepsilon q_n \alpha_{1\,n-1} + \ldots) e^{i(kx-\sigma t)}; \tag{2}$$

only the real part is of significance. In this specification,

$$\varepsilon^2 = \frac{2\nu_1 K^2}{\sigma_0}, \qquad q_n = \left(\frac{\nu_n}{\nu_1}\right)^{1/2}; \tag{3}$$

in (2), σ is developed in the form

$$\sigma = \sigma_0 + \varepsilon\sigma_1 + \ldots . \tag{4}$$

The quantity $\nu_n (n = 2, 3, \ldots . N)$ denotes the eddy viscosity in the thermocline layer between the $(n-1)^{\text{th}}$ and n^{th} sheets; ν_1 and ν_{N+1} are respectively the eddy viscosities in the layers above and below the thermocline. The fixed impermeable bottom is given by

$$y = -y_{N+1}, \tag{5}$$

and the free surface is given by the real part of

$$y = \eta_1 = ae^{i(kx-\sigma t)}. \tag{6}$$

The mass distribution is such that $\varrho_n (n = 2, 3, \ldots . N)$ is the density of the water in the homogeneous layer between the $(n-1)^{\text{th}}$ and n^{th} sheets; ϱ_1 and ϱ_{N+1} are respectively the densities above and below the thermocline.

In this formulation we have specified a decay of the wave amplitude with time, represented by the value of $\varepsilon\sigma_1$. However, the decay of the wave amplitude with distance is readily obtained from this by a simple energy-flux argument. If we suppose that σ is a specified quantity, we develop K in the form

$$K = K_0 + \varepsilon' K_1 + \ldots , \tag{7}$$

where

$$\varepsilon'^2 = \frac{2\nu_1}{\sigma} K_0^2. \tag{8}$$

To the first order of approximation, K_1 may be simply related to σ_1 by using the value of the inviscid group velocity, $\partial\sigma_0/\partial K_0$. In time, t, the mean energy density, which is proportional to the square of the wave amplitude, is transmitted a distance of $t\partial\sigma_0/\partial K_0$; and, by virtue of (2) and (4), its amplitude has decreased by a factor $\exp(2\,Im\,\varepsilon\sigma_1 t)$. On using (7) in (2), this must be equal to $\exp(-2\,Im\,\varepsilon' K_1 x)$, with $x = t\partial\sigma_0/\partial K_0$. Accordingly, we have

$$Im\,\varepsilon' K_1 = -Im\,\varepsilon\sigma_1 \Big/ \left(\frac{\partial\sigma_0}{\partial K_0}\right). \tag{9}$$

Then, if we define T as the time required for a decrease in the amplitude by a factor e^{-1} while X is the distance over which the amplitude decreases by a factor of e^{-1}, we have

$$X = \left(\frac{\partial\sigma_0}{\partial K_0}\right) T, \tag{10}$$

from which the spatial decay is readily deduced from the temporal decay. Restricting attention to a decay with time, we now use the results of Johns

and Cross (1969), who have shown how the values of σ_0, σ_1 and $\alpha_{0\,n-1}$, $\alpha_{1\,n-1}$ may be obtained. The general relations are not given, because we have particularized the problem by specifying that

$$\left.\begin{aligned} y_n - y_{n-1} &= \delta h; \quad n = 2, 3, \ldots N \\ y_{N+1} - y_N &= H. \end{aligned}\right\} \tag{11}$$

Accordingly, the top of the thermocline is at a mean depth, y_1, below the free surface, and the lowermost sheet of the thermocline is at a mean height, H, above the fixed bottom. Within the thermocline, the N-2 inner sheets are separated by a homogeneous layer of equilibrium thickness, δh. The density stratification is specified by prescribing a density change, $\Delta\varrho$, across the entire thermocline; the fine structure is such that this consists of a density jump, $\delta\varrho$, across each of the N sheets. We therefore have

$$\left.\begin{aligned} \varrho_{N+1} - \varrho_1 &= \Delta\varrho \\ \varrho_n - \varrho_{n-1} &= \delta\varrho; \quad n = 2, 3, \ldots N. \end{aligned}\right\} \tag{12}$$

Finally, the eddy viscosity above and below the thermocline and in all the thermocline layers is taken to be uniform and equal to ν, in which case

$$q_n = 1. \tag{13}$$

In this special case, Johns and Cross (1969) have shown that the sequence of quantities σ_0 and $\sigma_{0\,n-1}$ are expressed by:

$$\left.\begin{aligned} \sigma_0^2 (\cosh Ky_1 - \alpha_{01}) \operatorname{cosech} Ky_1 &= gK \\ \sigma_0 (\varrho_{n-1} G^+_{n-1} + \varrho_n G^-_n) &= -ag\,\delta\varrho\,\alpha_{0\,n-1}; \quad n = 2, 3, \ldots N+1, \end{aligned}\right\} \tag{14}$$

where

$$G^+_1 = \frac{a\sigma_0}{K} (1 - \alpha_{01} \cosh Ky_1) \operatorname{cosech} Ky_1, \tag{15}$$

$$\left.\begin{aligned} G^-_n &= -\frac{a\sigma_0}{K} (\alpha_{0\,n-1} \cosh K\delta h - \alpha_{0n}) \operatorname{cosech} K\delta h \\ G^+_n &= \frac{a\sigma_0}{K} (\alpha_{0\,n-1} - \alpha_{0n} \cosh K\delta h) \operatorname{cosech} K\delta h; \\ & n = 2, 3, \ldots N, \end{aligned}\right\} \tag{16}$$

and

$$G^-_{N+1} = -\frac{a\sigma_0}{K} \alpha_{0N} \coth KH. \tag{17}$$

The elimination of the $\alpha_{0\,n-1}$ from these relations leads to a polynomial equation of degree $N+1$ in σ_0^2. The roots of this equation give the possible

modes of oscillation. The same equation may be used to compute the inviscid group velocity, $\partial\sigma_0/\partial K$.

The sequence of the quantities σ_1 and $\alpha_{1\,n-1}$ are expressed by:

$$\left.\begin{aligned} &\varrho_1\mathcal{J}_2 - \left\{\frac{gK}{\sigma_0^2}\,\delta\varrho\sinh Ky_1 + \varrho_1\cosh Ky_1\right\}\mathcal{J}_1 = \frac{i}{2}\,\varrho_1 A_1^+ \\ &\varrho_2\,\mathrm{cosech}\,K\delta h\,\mathcal{J}_3 + \left\{\frac{gK}{\sigma_0^2}\,\delta\varrho - \varrho_2\coth K\delta h - \varrho_1\coth Ky_1\right\}\mathcal{J}_2 \\ &\qquad + \left(\varrho_1\,\mathrm{cosech}\,Ky_1 - \frac{2gK}{\sigma_0^2}\,\delta\varrho\,\alpha_{01}\right)\mathcal{J}_1 \\ &= \frac{i}{2}\left[\varrho_2\left\{A_2^+\,\mathrm{cosech}\,K\delta h - A_2^-\coth K\delta h\right\} - \varrho_1 A_1^+\coth Ky_1\right] \end{aligned}\right\} \quad (18)$$

$$\left.\begin{aligned} &\varrho_n\mathcal{J}_{n+1} + \left\{\frac{gK}{\sigma_0^2}\,\delta\varrho\sinh K\delta h - (\varrho_n+\varrho_{n-1})\cosh K\delta h\right\}\mathcal{J}_n \\ &\qquad + \varrho_{n-1}\mathcal{J}_{n-1} - \frac{2gK}{\sigma_0^2}\,\delta\varrho\sinh(K\delta h)\,\alpha_{0\,n-1}\mathcal{J}_1 \\ &= \frac{i}{2}\left\{\varrho_n A_n^+ + \varrho_{n-1}A_n^- - (\varrho_n A_n^- + \varrho_{n-1}A_{n-1}^+)\cosh K\delta h\right\}; \\ &\qquad n = 3, 4, \ldots N \end{aligned}\right\} \quad (19)$$

and

$$\left.\begin{aligned} &\left\{\frac{gK}{\sigma_0^2}\,\delta\varrho - (\varrho_{N+1}\coth KH + \varrho_N\coth K\delta h)\right\}\mathcal{J}_{N+1} \\ &\qquad + \varrho_N\mathcal{J}_N\,\mathrm{cosech}\,K\delta h - \frac{2gK}{\sigma_0^2}\,\delta\varrho\,\alpha_{0\,N}\mathcal{J}_1 \\ &= \frac{i}{2}\left[\varrho_{N+1}\left\{A_{N+1}^+\,\mathrm{cosech}\,KH - A_{N+1}^-\coth KH\right\}\right. \\ &\qquad \left. + \varrho_N\left\{A_N^-\,\mathrm{cosech}\,K\delta h - A_N^+\coth K\delta h\right\}\right], \end{aligned}\right\} \quad (20)$$

where

$$\left.\begin{aligned} \mathcal{J}_1 &= \frac{a}{K}\sigma_1 \\ \mathcal{J}_n &= \frac{a}{K}(\sigma_1\alpha_{0\,n-1} + \sigma_0\alpha_{1\,n-1}); \qquad n = 2, 3, \ldots N+1. \end{aligned}\right\} \quad (21)$$

The constants $A_n^{\pm}$ are

$$A_n^- = (1-i)(G_{n-1}^+ + G_n^-)\left(\frac{\varrho_{n-1}}{\varrho_n+\varrho_{n-1}}\right); \qquad n = 2, 3, \ldots N+1, \quad (22)$$

$$A_n^+ = (1 - i)(G_n^+ + G_{n+1}^-)\left(\frac{\varrho_{n+1}}{\varrho_n + \varrho_{n+1}}\right); \qquad n = 1, 2, \ldots N, \tag{23}$$

and

$$\left.\begin{aligned} A_1^- &= 0 \\ A_{N+1}^+ &= \frac{a\,\sigma_0}{K}\,\alpha_{0N}\,\operatorname{cosech} KH. \end{aligned}\right\} \tag{24}$$

This system of equations, then, may be solved by matrix inversion to obtain the quantity σ_1.

The earlier work of Johns and Cross has also led to a representation of the local velocity shear, $\partial u/\partial y$, in the thermocline sheets. In particular, the amplitude of the shear just below the $(n-1)^{\text{th}}$ sheet is

$$\left|\frac{\partial u_n^-}{\partial y}\right|_{y=-y_{n-1}} = \frac{K^2}{\varepsilon}\,|A_n^-|; \tag{25}$$

this is correct to the lowest order of approximation. This representation of the local velocity shear may now be used to calculate the local Richardson number, Ri, at the center of the n^{th} sheet. In the present case,

$$Ri = \frac{g}{\varrho_1}\,\frac{\delta\varrho}{2\,(2\nu/\sigma_0)^{1/2}}\Bigg/\left|\frac{\partial u_n^-}{\partial y}\right|^2_{y=-y_{n-1}}; \tag{26}$$

here we have specified that the density jump, $\delta\varrho$, occurs across a sheet thickness of $2(2\nu/\sigma_0)^{1/2}$.

The numerical value of Ri is crucial to questions concerning the breakdown of internal waves. Considering the results of Miles (1961, 1963), we suggest that internal waves will be dynamically stable if $Ri > 1/4$. However, if $Ri < 1/4$, then internal waves on the sheet become unstable, break, and lead to the generation of local turbulence. Numerical evaluations of Ri, using (26), are obtained later for internal waves in multisheeted thermocline structures, and the results are interpreted from the point of view of sheet stability. With this application in mind, we finally derive an expression for the vertically integrated initial mean-energy density of the internal wave motion. This may be calculated on the basis of the lowest-order inviscid theory outlined by Johns and Cross. The required quantity is expressed by

$$\left.\begin{aligned} E = {} & \frac{1}{4}\,g\,\varrho_1\,a^2 + \frac{1}{4}\,g\,\delta\varrho\,a^2 \sum_{n=2}^{N+1} \alpha_{0n-1}^2 \\ & + \frac{1}{4K}\,\varrho_1\,\sigma_0^2\,a^2\left\{(\alpha_{01}^2 + 1)\coth Ky_1 - 2\,\alpha_{01}\operatorname{cosech} Ky_1\right\} \end{aligned}\right\} \tag{27}$$

$$+\frac{1}{4K}\sigma_0^2 a^2 \sum_{n=2}^{N} \varrho_n \{(\alpha_{0n}^2 + \alpha_{0n-1}^2) \coth K\delta h - 2\alpha_{0n}\alpha_{0n-1} \operatorname{cosech} K\delta h\}$$
$$+\frac{1}{4K}\varrho_{N+1}\sigma_0^2 a^2 \alpha_{0N}^2 \coth KH. \qquad (27)$$

One of our objectives is concerned with the determination of the maximum value of E consistent with the stability of all the sheets in the thermocline structure. In particular, we are concerned with how this value varies with the addition of more sheets.

3. *Numerical Evaluation and Discussion.* As a numerical example, we have selected a single Fourier component of the internal wave spectrum that has a wave number $10^{-3}\,m^{-1}$; this corresponds to a wavelength of about 6.3 km. The depth, y_1, of the mean position at the top of the thermocline beneath the free surface is 50 m; the height, H, of the lowermost thermocline sheet above the bottom is 300 m, and the total thickness of the thermocline is 50 m. Thus the total depth is 400 m. These distances remain fixed throughout the numerical evaluation. The density change, $\Delta\varrho$, across the thermocline is

$$\frac{\Delta\varrho}{\varrho_1} = \frac{\varrho_{N+1}}{\varrho_1} - 1 = 0.002. \qquad (28)$$

As additional sheets are added to the structure, the density change across each of these sheets is expressed by

$$\delta\varrho = \Delta\varrho/N, \qquad (29)$$

where N is the total number of sheets in the thermocline. With N sheets, the value of δh is

$$\delta h = 50/(N-1)\ \text{m}. \qquad (30)$$

The basic value of ν is $1.4\times10^{-4}\,\text{m.}^2\text{s}^{-1}$, or about 100 times the basic value for the laminar flow of seawater.

The first quantity computed is the period of the possible internal modes of oscillation as a function of the number of sheets. To the first order of approximation in ε,

$$P = 2\pi/(\sigma_0 + Re\,\varepsilon\sigma_1), \qquad (31)$$

where σ_0^2 is one of the roots of the polynomial equation that is derived from (14)–(17). For the lower-order internal modes, the frictional correction to the inviscid wave period is negligibly small. For the higher-order modes, this correction plays an increasingly important role, so that, in the case of the seventh internal mode, it enhances the inviscid period by about 15%. The variation of P (in hours) with N is given in Fig. 1. For the first internal mode,

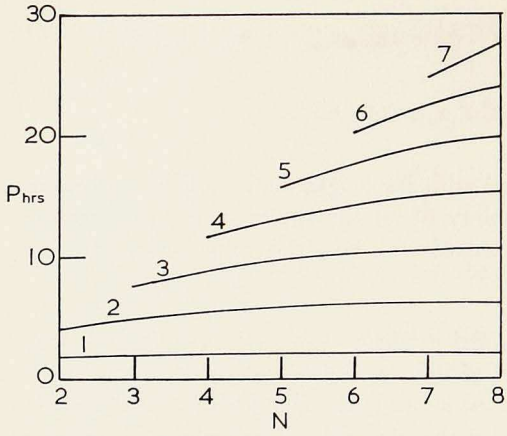

Figure 1. The period P, in hours, of the internal modes as a function of the number of sheets in the thermocline. The numbers refer to the order of the mode.

we observe that the wave period is effectively unaltered by the addition of more sheets to the structure. For the higher-order modes, however, the addition of more sheets leads to a progressive increase in the period of a specific mode. The range of wave periods extends from about 1.7 hours for the first internal mode to about 27.4 hours for the seventh internal mode.

We now compute the time, T (in hours), required for the amplitude of a wave mode to decrease by a factor e^{-1}. This quantity is expressed by

$$T = -1/Im\,\varepsilon\sigma_1. \tag{32}$$

Its value, for the first seven internal modes, is given as a function of N in Fig. 2. From this we are able to draw several interesting conclusions.

First, for a specified mode, the addition of more sheets actually leads to a decrease in the rate of energy dissipation; the internal waves are less heavily damped and persist as free oscillations for a longer time. This is contrary to our earlier speculations but may be explained as follows. In the case of a two-sheeted structure, the change in velocity across the thermocline takes place in two stages within the shear layers at each of the sheets. As more sheets are added, the velocity change occurs more gradually because of the introduction of more shear layers. Accordingly, the velocity shear in each of these decreases with an increase in the total number of sheets. Since the energy dissipation is determined by the mag-

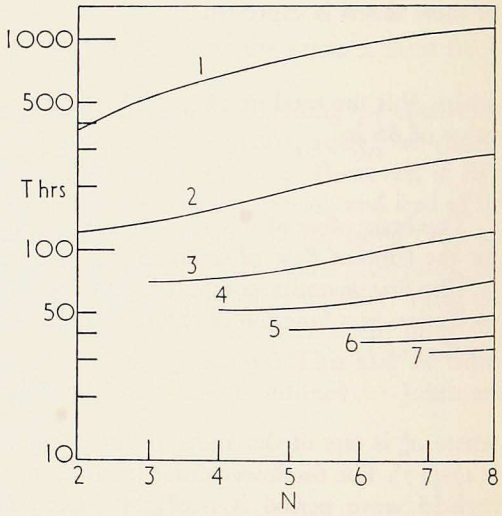

Figure 2. The time, T, in hours, required for the amplitudes of the internal modes to decrease by a factor e^{-1} expressed as a function of the number of sheets in the thermocline.

nitudes of the shears at the sheets, it is not unreasonable, therefore, to expect a decrease with the addition of more sheets.

Second, the higher-order internal modes are heavily damped in comparison with the lower modes. For example, in the case of an eight-sheeted structure, the fifth internal mode cannot exist as a free oscillation for more than about five cycles, by which time its amplitude will have decreased by a factor of e^{-2}. On the other hand, the first internal mode is virtually unaltered in this time. Reasons for this result can be found by physical argument. The m^{th} internal mode is characterized by m-1 changes in the phase of the vertical water velocity through the thermocline structure. For reasons of continuity, these changes must be accompanied by m changes in the phase of the horizontal velocity in the thermocline. Hence, for the larger values of m, significant shearing motions will be found throughout the entire depth of the thermocline structure. Accordingly, all the shear layers at the sheets will make major contributions to the energy dissipation, thus leading to a greatly enhanced rate of decay. By contrast, the first internal mode will induce high shears at only one level in the thermocline; consequently, the rate of decay will be much smaller. Given a thermocline structure of the type proposed in this paper, we may have an explanation as to why the lowest-order internal mode is the one most likely to be observed in practice.

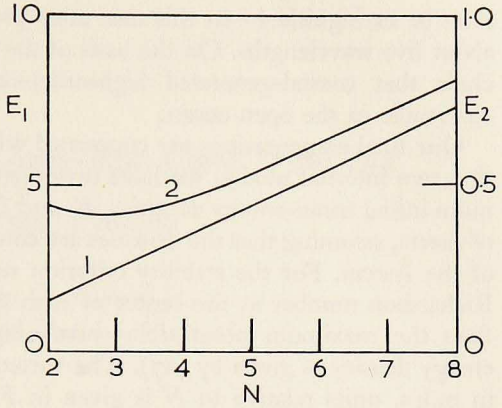

Figure 3. The energy densities E_1 and E_2, in m.k.s. units, for the first two internal modes expressed as functions of the number of sheets in the thermocline.

Considering the occurrence of internal wave modes in the deep ocean, it is also informative to interpret the above results in terms of a spatial attenuation. This may be deduced from eq. (10), in which the group velocity corresponds to a specified internal wave mode. In the present example, we find that, for the internal modes, the group velocity and phase velocity never differ by more than about 1%. Accordingly, we write

$$X \simeq \sigma_0 T/K. \tag{33}$$

In the case of a six-sheeted structure, we find that $X \simeq 3270$ km for the first internal mode and $X \simeq 15$ km for the fifth internal mode.

Hence, in theory the lowest-order mode can propagate a vast distance out to sea without suffering an amplitude decrement whereas the higher modes will

soon be extinguished—in this case after propagating over a distance equal to about five wavelengths. On the basis of the present model, then, we may conclude that coastal-generated high-order-mode internal waves will not be observable in the open ocean.

Our final computations are concerned with stability characteristics. For the first two internal modes, we have investigated the extent to which the maximum initial mean-energy densities, E_1 and E_2, are dependent upon the number of sheets, assuming that the densities are consistent with the dynamical stability of the system. For the stability criterion we assume that the minimum local Richardson number at the center of each sheet is never less than 0.25. This fixes the maximum permissible wave amplitude and hence the maximum energy density as given by (27). The variation in measurements of E_1 and E_2 in m.k.s. units relative to N is given in Fig. 3. Inspection of Fig. 3 reveals two principal results.

(i) The second mode is less stable than the lowest mode in terms of breakdown following a much smaller energy input. In fact, our calculations show that instabilities in the lowest mode occur at the lowermost sheet whereas instabilities in the second mode occur almost simultaneously at the top and bottom sheets. The amplitudes of the maximum vertical displacements associated with these energy densities are respectively of the order of 14 m and 7 m in the case of the two-sheeted structure.

(ii) The stability of a specified mode is ultimately increased by the addition of more sheets to the thermocline. Our results indicate that one extra sheet can increase the stability by as much as 100%. This conclusion does, of course, depend upon the uniformity of the coefficient of eddy viscosity and also upon the equal spacing of the sheets in the thermocline. However, the increased stability is so marked here that the general tendency may well be the same in less favorable circumstances.

REFERENCES

Johns, Bryan, and M. J. Cross
1969. The decay of internal wave modes in a multi-layered system. Deep-sea Res., *16*: 185–195.

Miles, J. W.
1961. On the stability of heterogeneous shear flows. J. fluid Mech., *10*: 496.
1963. On the stability of heterogeneous shear flows. Part 2. J. fluid Mech., *16*: 209–227.

Woods, J. D., and G. G. Fosberry
1967. The structure of the thermocline. Underwat. Ass. Rep., 1966–67: 5–17.

Sediment Budget in a Deep-Sea Core from the Central Equatorial Pacific[1]

G. Ross Heath, Theodore C. Moore, Jr.,
B. L. K. Somayajulu[2], and David S. Cronan[3]

Department of Oceanography
Oregon State University
Corvallis, Oregon 97331

ABSTRACT

Stratigraphic, mineralogic, chemical, and geochronologic measurements on a core from 8°20′N, 153°W show that sediment has been accumulating at a rate of 160 g/cm²/10⁶ years. Of this, 125 g is "fresh" Quaternary sediment while the remainder is lower and middle Tertiary material eroded from nearby outcrops. Comparison of the core with 37 others taken within a few kilometers indicates that the measured rate of accumulation has been at least an order of magnitude higher than the regional average. However, comparison with geochemical models suggests that the rate of accumulation in the core has been 1.4–3.5 times lower than the average for all pelagic sediments.

Introduction. During the 1965 WAHINE Expedition of the Scripps Institution of Oceanography, a small area southeast of Hawaii (8°20′N, 153′W; Fig. 1) was surveyed in detail. Thirty-eight closely spaced cores (Fig. 2) were collected from this area to evaluate the importance of local variability in the overall pattern of deep-sea sedimentation. The structural setting of the cores and the distribution of Quaternary sediments and manganese nodules have been discussed by Moore and Heath (1966, 1967). Subsequently, studies were made of the stratigraphy (Moore 1968, 1969), of the mineralogy (Heath 1968, 1969), and of the geochemistry (Cronan 1967, 1969b) of selected samples. The studies have clearly shown that the texture and mineralogy of the Quaternary sediment are fairly uniform (Table I) whereas its thickness varies by more than two orders of magnitude. The degree of contamination of Quaternary sediment by locally derived lower and middle Tertiary debris has also been highly variable (Table I).

1. Accepted for publication and submitted to press 12 February 1970.
2. Tata Institute of Fundamental Research, Homi Bhabha Road, Bombay-5, India.
3. Department of Geology, University of Ottawa, Ottawa 2, Ontario, Canada.

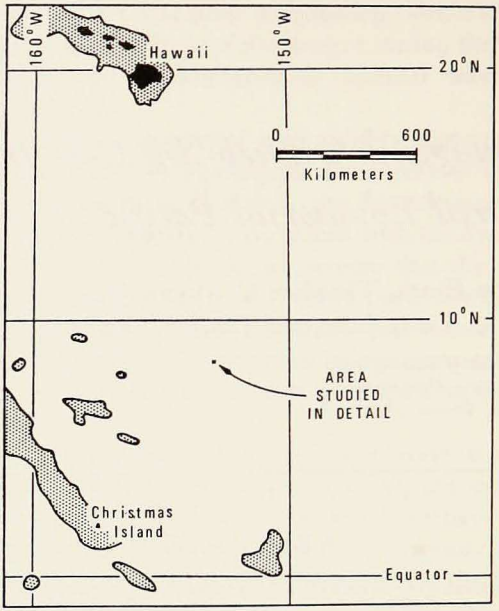

Figure 1. Location of study area (Fig. 2) containing core WAH 24F-8. Stippled areas indicate water that is shallower than 4 km.

If these findings are valid for large portions of the deep oceanic basins, it seems that isolated samples of deep-sea sediment can yield mineralogical data that are close to the average for large surrounding areas and can therefore be used to establish global distribution patterns (Biscaye 1965, Griffin et al. 1968). On the other hand, isolated data on mixing and rates of accumulation may deviate markedly from the local mean (Ku et al. 1968).

Recently, one of us (B. L. K. S.) has determined the rate of accumulation of sediment in core WAH 24F-8 (Fig. 2) by the ionium-thorium method (Goldberg and Koide 1962). The measurements (Fig. 3; Table II) indicate essentially uniform deposition throughout the interval sampled (72 cm). In this paper we use this determination to calculate the absolute rates of accumulation of selected components in the sediment of core WAH 24F-8. The regional validity of these rates can then be evaluated from our knowledge of the pattern of sedimentation in the surrounding area.

Results. The following experimental details of the techniques employed have been reported: the stratigraphic analyses and estimates of mixing (Moore 1968), the mineralogical and textural analyses (Heath 1968), the chemical analysis (Cronan and Tooms 1969), and the ionium-thorium dating (Goldberg and Koide 1962).

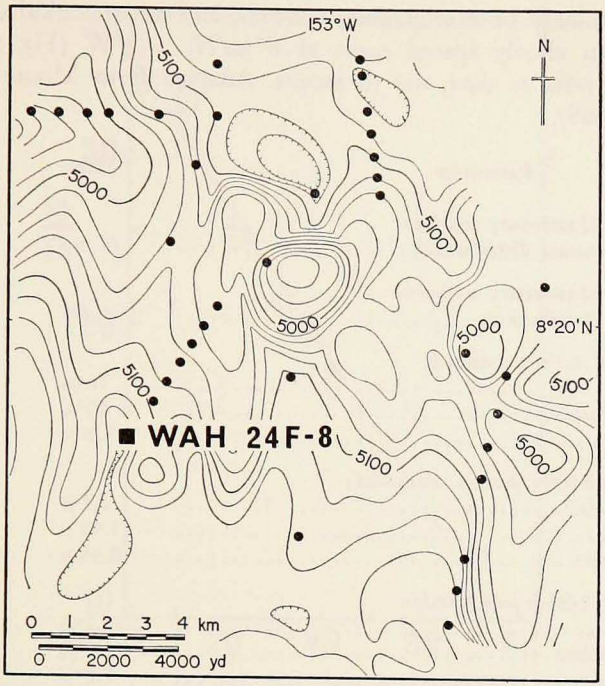

Figure 2. Topographic setting of core WAH 24F-8 and its relation to other nearby cores (solid dots). Contours in corrected meters: interval 20 m.

A straight line fitted by least squares to the ionium-thorium data (Fig. 3) yielded a rate of accumulation of 5.5 mm/1000 years (5.5 m/10^6 years). The wet density of the sediment in the core was very uniform (range: 1.20–1.22 g/cc). The mean accumulation rate of the solid phases was 0.16 g/cm^2/1000 years, or 160 g/cm^2/10^6 years.

Contamination of the Quaternary sediment by material eroded from nearby lower and middle Tertiary outcrops has been a complex function of topography, small-scale tectonics, and local variations in the pattern of sedimentation (Moore 1969). However, at a single location such as WAH 24F-8, the extent of mixing appears to have been remarkably uniform for a period of almost 200,000 years represented by the core (Table III). If the nonbiogenous components of the reworked Tertiary sediments were redistributed in the same way as the included microfossils, it is possible to calculate the rates at which "fresh" and reworked sediment have accumulated at WAH 24F-8 (Table III).

Cronan's (1967) analytical data for several elements in this core, together with the deduced rates of accumulation of the elements determined, are summarized in Table IV. The uniform mineralogy of samples from WAH 24F-8

Table I. Summary of stratigraphic, textural, and mineralogical data for sediment from closely spaced cores at 8°20'N, 153°W (Fig. 2). Standard deviations refer to data, not to means. Adapted from Moore (1968) and Heath (1968).

Parameter	Mean	Mean ± 1 standard deviation
*Thickness of Quaternary sediment (arithmetic normal distribution)	41 cm	4–77 cm
*Thickness of Quaternary sediment (log-normal distribution)	15 cm	2.7–76 cm
Components of surface sediment		
Quaternary	76%	59–94%
Oligocene-Miocene	18%	4–32%
Eocene	5.4%	0.5–10.3%
Grain-size parameters (Stokes diameters)		
25th percentile	5.7 μ	5.2–6.2 μ
Median	1.42 μ	1.34–1.51 μ
75th percentile	0.43 μ	0.41–0.45 μ
Mineralogy of 2-20-μ size fraction		
Quartz	12.1%	11.4–12.8%
Total plagioclase	11.5%	10.2–12.8%
Plagioclase An_{0-75}	8.3%	7.8– 8.8%
Pyroxene	3.4%	3.1– 3.7%
Mineralogy of < 2-μ size fraction		
Montmorillonite	46%	38–54%
Illite	36%	31–40%
Chlorite	11%	9–13%
Kaolinite	7%	6– 9%

* The distribution of thicknesses in Quaternary sediment is strongly positively skewed if treated as arithmetric normal but almost symmetrical if treated as log-normal. Thus, parameters derived from the latter treatment probably yield a better description of sedimentation in the area. Since the distribution is open (not all cores penetrated the full Quaternary section), statistical parameters have been derived graphically (Inman 1952).

and from other cores in the vicinity (Heath 1968) suggests that extrapolation of the results from a single analysis is justified.

The mineralogical data (Table V) refer either to the 2-20-μ or to the less-than-2-μ size fractions. Together, these two fractions form 90–92% of all samples. The boundary at 2 μ corresponds fairly closely to a natural break between the fine-grained clay minerals and the coarser more-equidimensional minerals like quartz, feldspars, and pyroxenes. The abundances of clay minerals in the less-than-2-μ fractions, estimated according to Biscaye's (1965) convention, may contain systematic errors (Biscaye 1965, Heath 1968). The 2-20-μ minerals, determined by X-ray diffraction, using an α-alumina inter-

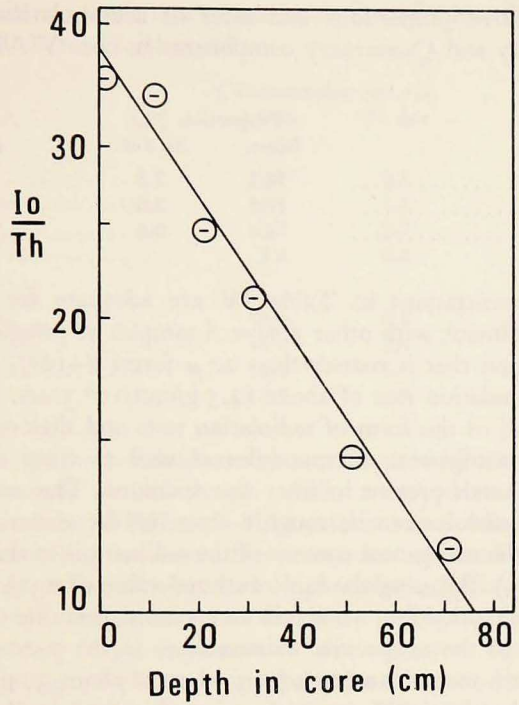

Figure 3. Logarithm of the activity ratio Io (Th^{230}): Th^{232} versus depth for core WAH 24 F-8. The least-squares-fit straight line is equivalent to an accumulation rate of 5.5 mm/1000 yrs.

nal standard, should be relatively free of systematic errors. The 2-20-μ material is probably largely of eolian origin (Rex and Goldberg 1958, Windom 1969) whereas the less-than-2-μ fraction could include nepheloid material introduced to the area by bottom currents (Jacobs and Ewing 1969).

Note that neither the mineralogy nor the chemistry of the sediment is fully defined. The abundances of the major elements—silicon, aluminium, the alkalis, alkali earths, and oxygen—have not been determined. However,

Table II. Thorium isotopes in sediment from core WAH 24F-8 (8° 18′ 16″N, 153° 02′ 50″W). Analysis by B. L. K. Somayajulu.

Sample interval (cm)	Th^{232} (ppm)	$\frac{Th^{230}}{Th^{232}}$	$\frac{Th^{228}}{Th^{232}}$
0– 2	5.5	35.1	1.31
10–12	5.3	33.8	1.00
20–22	3.8	24.6	1.02
30–32	5.6	21.0	1.00
49–53	2.7	14.4	1.12
70–72	3.7	11.6	1.08

Table III. Relative proportions and rates of accumulation of lower and middle Tertiary and Quaternary components in core WAH 24F-8. After Moore 1968.

Component	Proportion (%) Mean	St. dev.	Accumulation rate (g/cm²/10⁶ yrs.)
Quaternary	78.1	2.5	125
Oligocene-Miocene	17.5	2.0	28
Eocene	4.4	0.6	7

the element concentrations in Table IV are adequate for comparing the WAH 24F-8 sediment with other analyzed samples of pelagic deposits.

The size fraction that is coarser than 20 μ forms 8–10% of the sediment and has an accumulation rate of about 14.5 g/cm²/10⁶ years. This fraction is dominated by opal in the form of radiolarian tests and diatom frustules. Also present are ferromanganese micronodules as well as trace amounts of fish debris and of minerals present in finer-size fractions. The rate of accumulation of the micronodules can be roughly estimated by assuming that approximately 88% of the manganese content of the sediment is in this form (Chester and Hughes 1966). By using the same authors' value of 23% for the manganese content of micronodules, we obtain an accumulation rate of 6.2 g/cm²/10⁶ years. The bulk of the unspecified minerals are in the 2-20-μ size fraction, of which they form more than 60% (equivalent to about 30 g/cm²/10⁶ years). Clay minerals, the dominant components of this "missing" material, could not be reliably estimated because grains of opal and other more or less equidimensional minerals interfered with the preparation of consistently oriented aggregates for X-ray diffraction analysis. Although the precision of the estimates is poor, it appears that the only major difference between the relative proportions of the principal clay minerals in the 2-20-μ and less-than-2-μ fractions is a reduction of montmorillonite by 30–50% in the coarser material.

Table IV. Analytical data at 58–60 cm and rate of accumulation of trace elements in core WAH 24F-8.

Element	Concentration (wt. %)	Accumulation rate (g/cm²/10⁶ yrs.)
Fe	3.45	5.5
Mn	1.02	1.6
Ni	0.05	0.08
Co	0.01	0.02
Cu	0.02	0.03
Pb	0.002	0.003
V	0.02	0.03
Cr	0.005	0.008
Ti	0.30	0.48
P	0.09	0.14
Mo	0.004	0.006

Discussion. The data for WAH 24F-8 (Tables III–V) are strictly applicable to only the few square centimeters sampled by the coring tube. To what extent can these data be extrapolated to the surrounding few square kilometers shown in Fig. 2, or even

Table V. Abundances and rates of accumulation of selected minerals in core WAH 24F-8. After Heath 1968.

Mineral	Concentration (wt. %) Mean	St. dev	Accumulation rate ($g/cm^2/10^6$ yrs.)
2-20-μ fraction			
Quartz	12.2	0.4	6.0
Total plagioclase	11.8	1.1	5.8
Plagioclase An_{0-75}	8.8	0.7	4.4
Pyroxene	3.8	0.3	1.9
<2-μ fraction			
Montmorillonite	30.4	3.3	29.1
Illite	44.5	2.4	42.6
Chlorite	15.3	0.4	14.6
Kaolinite	9.7	0.5	9.3

to the surrounding few hundred or thousand square kilometers? If the data in Table I constitute a valid sample of the surveyed area, it appears that the constitution of the WAH 24F-8 material is not markedly different from that in the surrounding sediment. However, the measured rate of accumulation is at least an order of magnitude higher than the local average (if the distribution of sediment thicknesses is taken to be log normal; Table I). Because of the very large dispersion of the thickness data, it is doubtful whether the existing sample coverage forms an adequate basis for estimating an "average" rate of deposition for the area. What these data do point to, however, is the difficulty of using the budget for WAH 24F-8, or for any other isolated core, as a basis for calculating meaningful rate constants and partition coefficients for the geochemical cycle.

By comparing the element concentrations in Table IV with the averages of Goldberg and Arrhenius (1958) and Cronan (1969b) and with the values derived from mass-balance calculations by Horn and Adams (1966), we see that the WAH 24F-8 sediment is close to a "typical" pelagic clay. Only Mn, Ni, and Mo are somewhat anomalous in that they are slightly enriched in this core relative to their average abundances in pelagic clays. This enrichment may reflect the presence of the ferromanganese micronodules mentioned previously, since Ni and Mo seem to be concentrated in this phase (Cronan 1969a).

If this core does represent "typical" pelagic sediment, what does the budget reveal about published geochemical material balances? Let us consider only the models of Goldberg and Arrhenius (1958) and Horn and Adams (1966), since their results are fairly close to the published extremes. Horn and Adams have concluded that the abundance and distribution of elements in various types of sediment and in the ocean result from the weathering of 2.04×10^{24} g of crustal igneous rock whereas Goldberg and Arrhenius have arrived at an estimate of 9.4×10^{23} g. Horn and Adams have assumed that the amount of

pelagic clay is 86% of 3.38×10^{23} g and that this is deposited over an area of 2.68×10^{18} cm^2 (about 53% of the earth's surface). This is equivalent to 1.1×10^5 g/cm^2. Goldberg and Arrhenius have arrived at a mass of pelagic sediments of 2.3×10^4 g/cm^2 for the entire earth, equivalent to 4.4×10^4 g/cm^2 for the area used by Horn and Adams.

Our value of 125 g/cm^2/10^6 years for Quaternary (i.e., "fresh") material deposited at WAH 24F-8 yields periods of accumulation of 350 million years (Goldberg and Arrhenius 1958) and 870 million years (Horn and Adams, 1966). Since neither of the models under consideration is concerned with recycled components, the period of accumulation should refer to the present reservoir of pelagic sediment.

The distribution and age of ancient pelagic sediments (Ewing et al. 1966, Riedel 1970) in combination with recent advances in our understanding of global tectonics (Isacks et al. 1968, Le Pichon 1968, Heirtzler et al. 1968) suggest that the lifetime of the pelagic reservoir should be no more than 200 miilion years.

The excessive ages derived from the geochemical models could be explained by systematic errors in their compositional values. Since few analytical data are available for pre-Quaternary sediments, recent changes in the abyssal regions would introduce errors that could invalidate the mass terms of a geochemical balance. It is more likely, however, that the excessive ages calculated from the Goldberg-Arrhenius and Horn-Adams models indicate a slower-than-average rate of accumulation at WAH 24F-8.

If we take the lifetime of the pelagic reservoir to be 200 million years and assume that it covers an area of 2.68×10^{18} cm^2 (Horn and Adams 1966), the mean rate of sedimentation of new pelagic sediment must be 180 g/cm^2/10^6 years to satisfy the Goldberg-Arrhenius model and 440 g/cm^2/10^6 years to satisfy the Horn-Adams model. In other words, the accumulation rate in core WAH 24F-8 is 1.4–3.5 times lower than the average for all pelagic sediments.

Since we have already concluded that the sedimentation rate at this site is anomalously high compared with nearby cores, it appears that sediment in the surveyed area is accumulating between one and two orders of magnitude more slowly than in the pelagic realm as a whole. It is not clear whether this results from a lower-than-average supply of sediment or whether a major fraction of the sediment reaching the area is carried away by the northward-moving Antarctic Bottom Water (Lynn and Reid 1968).

Acknowledgments. Financial support from the Office of Naval Research [contracts Nonr 2216(05), Nonr 2216(23) and NR 260-103], from National Science Foundation (grants GP 2873 and 2891), and from the International Nickel Company, covering portions of this research, is gratefully acknowledged.

REFERENCES

BISCAYE, P. E.
1965. Mineralogy and sedimentation of recent deep-sea clay in the Atlantic Ocean and adjacent seas and oceans. Bull. geol. Soc. Amer., *76*: 803–832.

CHESTER, ROY, and M. J. HUGHES
1966. The distribution of manganese, iron and nickel in a North Pacific deep-sea clay core. Deep-sea Res., *13*: 627–634.

CRONAN, D. S.
1967. The geochemistry of some manganese nodules and associated pelagic deposits. Ph.D. thesis, University of London; 342 pp.
1969a. Inter-element associations in some pelagic deposits. Chem. Geol., *5*: 99–106.
1969b. Average abundances of Mn, Fe, Ni, . . . in Pacific pelagic clays. Geochim. Cosmochim Acta, *33*: 1562–1565.

CRONAN, D. S., and J. S. TOOMS
1969. The geochemistry of manganese nodules and associated pelagic deposits from the Pacific and Indian oceans. Deep-sea Res., *16*: 335–359.

EWING, MAURICE, T. SAITO, J. I. EWING, and L. H. BURCKLE
1966. Lower Cretaceous sediments from the northwest Pacific. Science, *152*: 751–755.

GOLDBERG, E. D., and G. O. S. ARRHENIUS
1958. Chemistry of Pacific pelagic sediments. Geochim. Cosmochim. Acta, *13*: 153–212.

GOLDBERG, E. D., and M. KOIDE
1962. Geochronological studies of deep sea sediments by the ionium/thorium method. Geochim. Cosmochim. Acta, *26*: 417–450.

GRIFFIN, J. J., H. L. WINDOM, and E. D. GOLDBERG
1968. The distribution of clay minerals in the world ocean. Deep-sea Res., *15*: 433–459.

HEATH, G. R.
1968. Mineralogy of Cenozoic deep-sea sediments from the equatorial Pacific Ocean. Univ. Calif. San Diego, Scripps Inst. Oceanogr., Ph.D. Dissertation; 168 pp.
1969. Mineralogy of Cenozoic deep-sea sediments from the equatorial Pacific Ocean. Bull. geol. Soc. Amer., *80*: 1197–2018.

HEIRTZLER, J. R., G. O. DICKSON, E. M. HERRON, W. C. PITTMAN III, and X. LE PICHON
1968. Marine magnetic anomalies, geomagnetic field reversals, and motions of the ocean floor and continents. J. geophys. Res., *73*: 2119–2136.

HORN, M. K., and J. A. S. ADAMS
1966. Computer-derived geochemical balances and element abundances. Geochim. Cosmochim. Acta, *30*: 279–297.

INMAN, D. L.
1952. Measures for describing the size distribution of sediments. J. sediment. Petrol., *22*: 125–145.

ISACKS, BRYAN, JACK OLIVER, and L. R. SYKES
1968. Seismology and the new global tectonics. J. geophys. Res., *73*: 5855–5899.

JACOBS, M. B., and MAURICE EWING
1969. Suspended particulate matter: concentration in the major oceans. Science, *163*: 380–383.

Ku, Teh-Lung, W. S. Broecker, and Neil Opdyke
1968. Comparison of sedimentation rates measured by paleomagnetic and the ionium methods of age determination. Earth planet. Sci. Letters, *4*: 1–16.

Le Pichon, Xavier
1968. Sea-floor spreading and continental drift. J. geophys. Res., *12*: 3661–3697.

Lynn, R. J., and J. L. Reid
1968. Characteristics and circulation of deep and abyssal waters. Deep-sea Res., *15*: 577–598.

Moore, T. C., Jr.
1968. Deep-sea sedimentation and Cenozoic stratigraphy in the central equatorial Pacific. Univ. Calif. San Diego, Scripps Inst. Oceanog., Ph.D. Dissertation; 129 pp.
1969. Abyssal hills in the central equatorial Pacific: sedimentation and stratigraphy. Deep-sea Res., *17*.

Moore, T. C., Jr., and G. R. Heath
1966. Manganese nodules, topography and thickness of Quaternary sediments in the central Pacific. Nature, London, *212*: 983–985.
1967. Abyssal hills in the central equatorial Pacific: detailed structure of the sea floor and subbottom reflectors. Mar. Geol., *5*: 161–179.

Rex, R. W., and E. D. Goldberg
1958. Quartz contents of pelagic sediments of the Pacific Ocean. Tellus, *10*: 153–159.

Riedel, W. R.
1970. Occurrence of pre-Quaternary Radiolaria in deep-sea sediments, *In*: SCOR Symposium on Micropaleontology of Marine Bottom Sediments. In press.

Windom, H. L.
1969. Atmospheric dust records in permanent snow-fields: implications to marine sedimentation. Bull. geol. Soc. Amer., *80*: 761–782.